# Generalized Predictive Control for Superheated Steam Temperature Regulation in a Supercritical Coal-fired Power Plant

Mihai Draganescu, Shen Guo, Jacek Wojcik, Jihong Wang, *Senior Member, IEEE, Member, CSEE*, Xiangjie Liu, *Senior Member, IEEE*, Guolian Hou, Yali Xue, and Qirui Gao

***Abstract*—The design and implementation of a Generalized Predictive Control (GPC) strategy for the superheated steam temperature regulation in a supercritical (SC) coal-fired power plant is presented. A Controlled Auto-Regressive Moving-Average (CARMA) model of the plant is derived from using the experimental data to approximately predict the plant's future behavior. This model is required by the GPC algorithm to calculate the future control inputs. A new GPC controller is designed and its performance is tested through extensive simulation studies. Compared with the performance of the plant using a conventional PID controller, the steam temperature controlled by the GPC controller is found to be more stable. The stable steam temperature leads to more efficient plant operation and energy saving, as demonstrated by the simulation results. Plant performance improvement is also tested while the plant experiences the load demand changes and disturbances resulting from the malfunctioning of coal mills.**

***Index Terms*—CARMA model, coal mill, GPC, load demand, PID, SC power plant, steam temperature control, superheater (SH).**

## I. Introduction

STEAM temperature control at the Superheater's (SH) outlet is one of the most important and challenging control tasks in a fossil fueled power plant. The temperature control is achieved by regulating the spray of water in a SH. The difficulty presents at high nonlinear characteristics of the SH, the extended time delays caused by the nature of the thermal process, and disturbances from the flue gases [1], [2]. In a coal-fired power plant, the higher steam temperature will lead to higher power plant efficiency. However, the plant can operate at a high temperature only when it is maintained at a stable level. Moreover, keeping the steam temperature stable prolongs the lifetime of the boiler and steam turbine while minimizing thermal stresses [2].

In order to reduce $CO_2$ emissions, power generation from intermittent renewable energy sources has grown dramatically over the past five years, forcing changes in the operating requirements of conventional power plants [3]. Although a plant is initially designed to operate at its base load, it needs to be flexible, efficient, and capable of handling changes in load demand and variations in power generation profiles from renewable energy [2]. This, in turn, makes it more difficult to maintain the steam temperature at a relatively constant value.

The most widely used controller in power plants is still the Proportional-Integral-Derivative (PID) controller because of its acceptable degree of control performance, simplicity, technology maturity, operation security, and robustness [4]. However, due to new challenges in keeping up with rapid changes in load demand and the transients, performance of the PID controller is far from being optimal [5]. This motivates the development of other type of controllers, such as model-based controllers.

Model Predictive Control (MPC) defines a class of control algorithms that calculates a series of control inputs based on the predicted behavior of process outputs over a time horizon. In an MPC algorithm, future control inputs are calculated in order to minimize the difference between the predicted control outputs and the set-point values over the prediction horizon. Only the first element of the calculated sequence of the control inputs is then applied to the calculation process. This process is repeated at subsequent sampling times with prediction horizons of the same length, but shifted one step forward. This process is termed the principle of a receding horizon [6].

Different predictive control algorithms have been developed over time. The Model Predictive Heuristic Control (MPHC) algorithm was first developed by Richalet *et al.* [7], which was followed later by a number of other such algorithms, including Dynamic Matrix Control (DMC), Quadratic Dynamic Matrix Control (QDMC) [8], Generalized Predictive Control (GPC) [9], and Shell Multivariable Optimizing Controller (SMOC) [10]. All these algorithms make use of linear process models to predict the future moves of the control variables. It has been demonstrated that the predictions made via the linear model are effective in calculating the next values for the control variables.

Manuscript received November 13, 2014; revised February 2, 2015 and February 22, 2015; accepted February 25, 2015. Date of publication March 30, 2015; date of current version March 19, 2015. The work was supported by the EPSRC Grant (EP/G062889/2), Advantage West Midlands and the European Regional Development Agency (Birmingham Science City Energy Efficiency & Demand Reduction project). Thanks are also due to the funding support and technical advice from E.ON Engineering (UK).

M. Draganescu, S. Guo, J. Wojcik and J. H. Wang (corresponding author, email: jihong.wang@warwick.ac.uk) are with the School of Engineering, University of Warwick, United Kingdom.

X. J. Liu and G. L. Hou are with the The State Key Laboratory of Alternate Electrical Power System with Renewable Energy Sources North China Electric Power University, Beijing, 102206, P.R. China.

Y. L. Xue and Q. R. Gao are with the School of Thermal Engineering, Tsinghua University, Beijing, China.

Digital Object Identifier 10.17775/CSEEJPES.2015.00009

A DMC controller for steam temperature control was developed in [2] and tested in a power plant simulator and in a field operating coal-fired power plant having a drum boiler. Simulation tests showed that the DMC control strategy outperformed the PID based controllers. A successful implementation of a DMC controller for steam temperature regulation is reported in [11], in which the controller was tested in a power plant simulator operating with a once-through boiler. Sanchez *et al.* [12] developed a DMC and a fuzzy controller to regulate the steam temperature in a 300 MW power plant simulator. The controllers' performance was compared to an existing PID, and the test results showed tighter temperature control when advanced control strategies were used. DMC has been successfully implemented and tested for coal milling process control in the authors' previous work [13]. However, there exist no reports of DMC applications to SH control for supercritical once-through boilers in the literature.

Clarke *et al.* [9] developed a GPC algorithm, which became popular both in industry applications, as well as in academic studies [14]. A key feature of the GPC algorithm is that it can be used with unstable and non-minimum phase plants [15]. In [16], the GPC controller shows good performance against the existing PID controller for regulating the superheated steam temperature in a real coal-fired power plant having a once-through boiler. For this reason, GPC is the method of choice for this research for addressing the new challenges faced by SH control with uncertain load demand profiles.

This paper presents the research in the development of a GPC for controlling once-through supercritical power plant SH. Section II begins with a description of the power plant, followed by a mathematical model and its implementation on a simulator. A SH PID controller implementation in a complex power plant process is explained in Section III. The procedures for design of the GPC controller are presented in the paper. The details of the algorithm and the structure of the GPC controller are presented. The simulation study is carried out to verify the GPC controller and the simulation results demonstrated the major improvement in plant dynamic performance.

## II. Description of the Power Plant Simulator

### A. Description of the SC Power Plant

Fig. 1 shows the simplified diagram of a super-critical (SC) coal-fired power plant, which illustrates the most significant components and the relationships between them.

A SC coal-fired power plant process is described as follows [15]. Chemical energy released from combustion is converted to thermal energy in the furnace. Released heat is exchanged between hot flue gases and working fluid through heat exchangers in the boiler: economizer, waterwall, primary SH, platen SH, final SH, and reheaters. Since the feedwater pressure is above the critical point, the sub-cooled water is converted to SC steam in the SHs without evaporation. The SC steam is then expanded through turbines. The high pressure (HP) turbine is energized by the steam supplied by Final SH, and the reheaters are used to recover energy by reheating

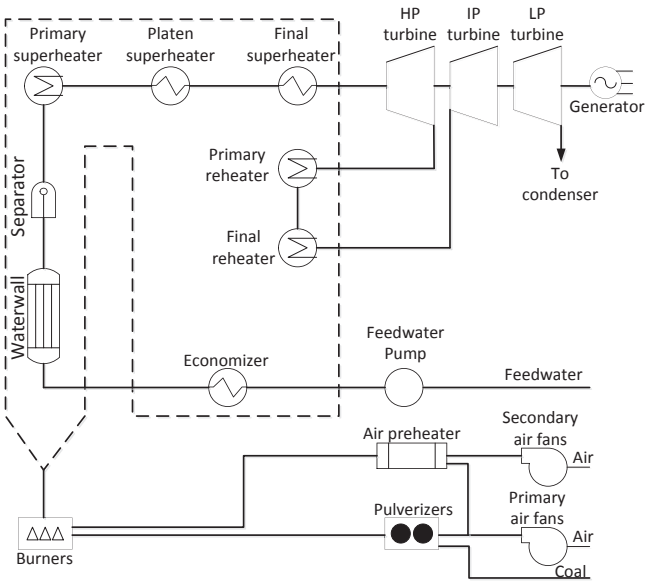


Fig. 1. Simplified diagram of a SC coal-fired power plant.

the exhaust steam from the HP turbine before it returns to the intermediate pressure (IP) and low pressure (LP) turbine. The mechanical power is converted to electrical power by the synchronous generator coupled to the turbine shaft. For the work described in the paper, the boiler specifications at the boiler rated load are shown in Table AI in Appendix.

### B. Mathematical Model of Power Plant

Detailed descriptions of the model derivation and parameters identification are reported in our previous work [16]–[18]. The SC boiler model is developed by deriving the nonlinear dynamic relationships of pressure and temperature in each heat exchanger from mass and energy balance equations of a certain control volume. Those equations are strongly coupled by the equations of SC steam flow and heat flow in the boiler. The heat flow is directly related to the fuel combustion. The boiler model parameters are initially calculated from steam tables and then identified using the data from certain operating unit responses. The former method is based on the steady states operation, and the latter approach has been adopted with the real power plant on-site measurement data. The steam turbine stages are modeled by the same principles of energy conservation and simply linked to the boiler model. The generator model [19], [20] has been coupled to the turbine model through torque equilibrium with other algebraic equations. The model has two direct inputs—feedwater flow and fuel flow and one indirect input, which is the valve position reference. The boiler turbine generator model has $20^{\text{th}}$ order rooted from its physical and engineering principles. It is then coupled to a vertical spindle mill model [16] to represent the power generation process from fuel preparation to electricity generation. Fig. 2 shows the model blocks diagram with all combined subsystems and the symbols are listed in Table AII in Appendix. The mathematical model is a simplified model, with which the initial controller design ideas can be tested.

Due to the complexity of the power generation process and

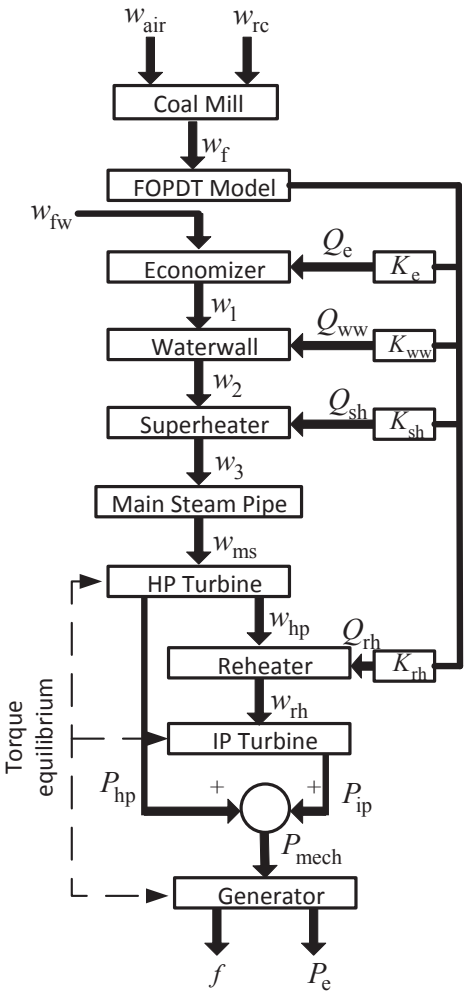


Fig. 2. Structure of the power plant mathematical model.

safety concerns, it is almost impossible to test new controllers on-line without passing a series of off-line tests to ensure that no cause damages/incidents will occur to the real power plant. The initial design procedure and simulation, thus has been carried out with the simplified power plant model. To conduct the off-line test in operating conditions close to a real power plant, jointly with Tsinghua University, a more detailed simulation model for a 600 MW SC power plant is developed at Warwick and implemented by modifying a power plant simulator in the research laboratory as shown in Fig. 3, which was initially developed for operators' training purposes. The mathematical model of the power plant was translated into FORTRAN code and then integrated into SimuEngine, a visual simulation support system.

## III. Description of the Superheater

### A. SH Process in the Simulator

The structure of the SH used in the power plant simulator, together with the process inputs and outputs is illustrated in Fig. 4. The SH is a heat exchanger with the function of transferring the heat from the flue gases to the steam coming from the waterwall, thus increasing the steam temperature. The


Fig. 3. Several GUI screens from the power plant simulator.

increased temperature means that more energy is available to be used by the turbine for conversion to mechanical and then electrical energy. Due to this added energy, the efficiency of the entire cycle is increased [21].

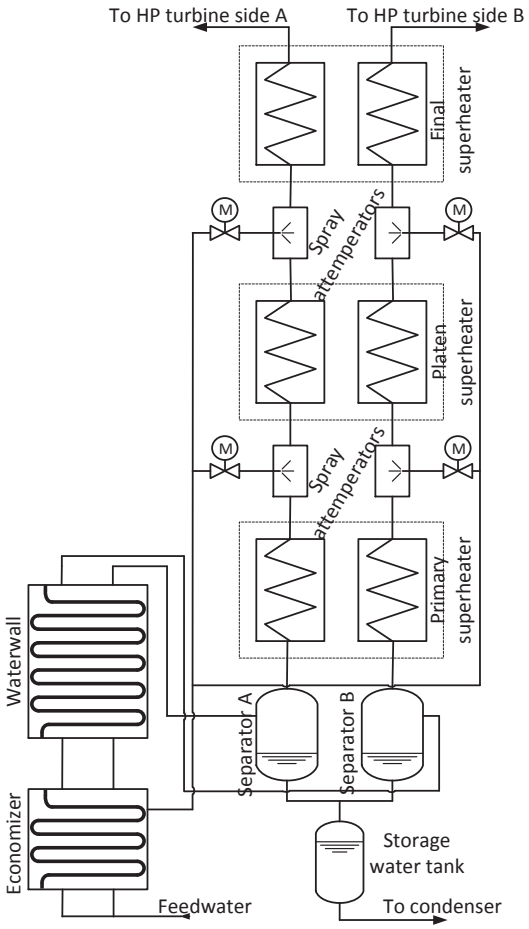


Fig. 4. Diagram of the SH modeled in the power plant simulator.

The efficiency of the turbine over a wide load range is affected, if the steam temperature is not maintained constant over that range [21].

The predominant method used to control steam temperature is attemperation using a device called a spray-type attemperator. Water is sprayed into the steam, forming steam through

evaporation, leading to the temperature of the final mixture being lower than the initial one [21].

The SH from the simulator has three sections: primary SH, platen SH and final SH. Each section is divided into two subsections, such that there are two steam paths going through the SH, denoted as A and B in Fig. 4. There are two attemperators on each side, one after primary SH and one after platen SH. The first attemperator is controlling the steam temperature at the outlet of the platen SH and the second attemperator is regulating the steam temperature at the outlet of the final SH.

### B. Existing Steam Temperature Control Structure

The temperatures at the outlet of platen SH and final SH are controlled by independent proportional-integral (PI) cascade control structures. Such a control structure is illustrated in Fig. 5.

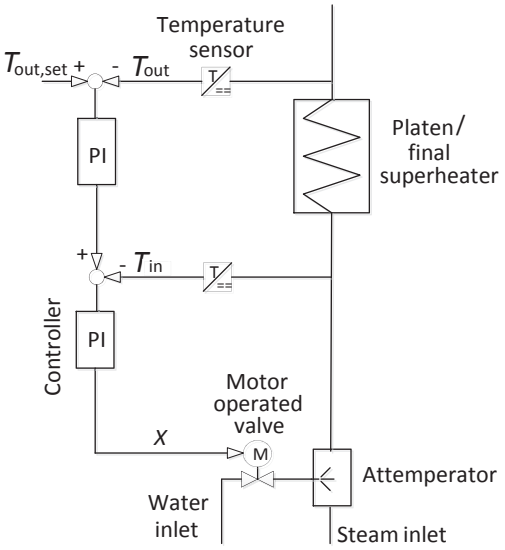


Fig. 5. Existing PI cascade control structure.

A PI cascade control structure uses an additional internal feedback loop to reject disturbances more effectively [22].

When the valve position of the attemperator changes, the spray water pressure changes as well and as a result, the spray water flow rate will be disturbed [23].

This disturbance can be rejected by using a PI cascade structure. Referring to Fig. 5, the control signal sent by the outer PI controller acts as the set-point for the inner control loop. In this loop, the temperature at the attemperator outlet is measured and the PI controller acts in such a way as to reduce the deviation between the set-point temperature from the outer controller and the temperature at the attemperator outlet. Because the inner loop is faster than the outer loop, the disturbance is rejected.

## IV. Generalized Predictive Controller Design

The most important temperature to be controlled is the steam temperature at the output of the last stage of the SH, namely, at the final SH outlet, just before entering the HP turbine [1].

The aim of this research work is to replace the PI cascade control loop, which controls the steam temperature at the outlet of the final SH with a controller based on a GPC algorithm. The block diagram of the GPC based steam temperature control is illustrated in Fig. 6, where $T_{\mathrm{set,out}}$ is the set-point temperature, $T_{\mathrm{out}}$ is the temperature at the final SH outlet, and $\delta$ is the valve position of the attemperator.

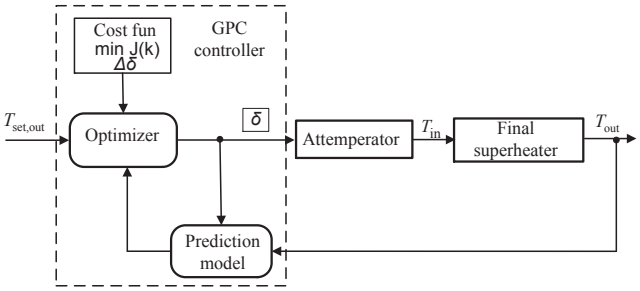


Fig. 6. Final SH temperature control loop based on GPC controller.

*1) Prediction Model:* The process to be controlled is a single-input single-output (SISO) process. The predictive controller is designed following the GPC algorithm for a SISO process, as presented in [11] and [23], [24].

For a SISO process, the discretized model linearized at a certain operating point, can be described by the following CARMA form:

$$A(z^{-1})y(t) = z^{-d}B(z^{-1})u(t-1) + C(z^{-1})\varepsilon(t), \qquad (1)$$

where $u(t)$ and $y(t)$ are the control and output sequences of the plant, $d$ is the dead time of the system, and $\varepsilon(t)$ is zero mean white noise. $A$, $B$ and $C$ are polynomials in the backward shift operator $z^{-1}$, as follows:

$$\begin{aligned} A(z^{-1}) &= 1 + a_1 z^{-1} + a_2 z^{-2} + \cdots + a_{na} z^{-na} \\ B(z^{-1}) &= b_0 + b_1 z^{-1} + b_2 z^{-2} + \cdots + b_{nb} z^{-nb} \\ C(z^{-1}) &= 1 + c_1 z^{-1} + c_2 z^{-2} + \cdots + c_{nc} z^{-nc}. \end{aligned} \qquad (2)$$

*2) Output Predictions:* The GPC algorithm predicts the value of the $(t+j)$th output by using past values of the input and output variables. The following Diophantine equation is considered:

$$1 = E_j(z^{-1})\widetilde{A}(z^{-1}) + z^{-j}F_j(z^{-1}), \qquad (3)$$

where $\widetilde{A}(z^{-1}) = \Delta A(z^{-1})$ and $\Delta = 1 - z^{-1}$.

The polynomials $E_j$ and $F_j$ are individually defined with degrees of $j-1$ and $na$, respectively. They can be obtained by dividing 1 by $\widetilde{A}(z^{-1})$ until the remainder can be factorized as $z^{-j}F_j(z^{-1})$. The quotient of the division is the polynomial $E_j(z^{-1})$. If (1) is multiplied by $\Delta E_j(z^{-1})z^j, y(t+j)$ can be obtained as:

$$\begin{aligned} y(t+j) = {} & F_j(z^{-1}y(t)) + \cdots \\ & + E_j(z^{-1})B(z^{-1})\Delta u(t+j-d-1) + \cdots \\ & + E_j(z^{-1})B(z^{-1})\Delta u(t+j-d-1) + \cdots \\ & + E_j(z^{-1})\varepsilon(t+j). \end{aligned} \qquad (4)$$

The prediction of $y(t+j)$ at the time $t$ becomes

$$\hat{y}(t+j|t) = G_j(z^{-1})\Delta u(t+j-d-1) + F_j(z^{-1})y(t), \quad (5)$$

where $G_j(z^{-1}) = E_j(z^{-1})B(z^{-1})$.

The polynomials $E_j(z^{-1})$ and $F_j(z^{-1})$ can be expressed as:

$$\begin{aligned} F_j(z^{-1}) &= f_{j,0} + f_{j,1}z^{-1} + \cdots + f_{j,na}z^{-na} \\ E_j(z^{-1}) &= e_{j,0} + e_{j,1}z^{-1} + \cdots + e_{j,j-1}z^{-(j-1)}. \end{aligned} \quad (6)$$

The polynomial $E_{j+1}(z^{-1})$ will be given by

$$E_{j+1}(z^{-1}) = E_j(z^{-1}) + e_{j+1,j}z^{-j}, \quad (7)$$

where $e_{j+1,j} = f_{j,0}$. The coefficients of polynomial $F_{j+1}(z^{-1})$ can be expressed as:

$$f_{j+1,i} = f_{j,i+1} - f_{j,0}\widetilde{a}_{i+1} \quad i = 0, \cdots, na-1. \quad (8)$$

The polynomial $G_{j+1}(z^{-1})$ can be obtained recursively as follows:

$$\begin{aligned} G_{j+1}(z^{-1}) &= E_{j+1}(z^{-1})B(z^{-1}) \\ &= [E_{j+1}(z^{-1}) + f_{j,0}z^{-j}]B(z^{-1}) \\ &= G_j(z^{-1}) + f_{j,0}z^{-j}B(z^{-1}). \end{aligned} \quad (9)$$

The first $j$ coefficients of $G_{j+1}(z^{-1})$ will be identical to those of $G_j(z^{-1})$ and the remaining coefficients will be given by:

$$g_{j+1,j+i} = g_{j,j+i} + f_{j,0}b_i \quad i = 0, \cdots, nb. \quad (10)$$

The vector $y$ of $N$ ahead predictions can be written as:

$$\mathbf{y} = \mathbf{G}\mathbf{u} + \mathbf{F}(z^{-1})y(t) + \mathbf{G}'(z^{-1})\Delta u(t-1), \quad (11)$$

where

$$\mathbf{y} = \begin{bmatrix} \hat{y}(t+d+1|t) \\ y(t+\hat{d}+2|t) \\ \vdots \\ \hat{y}(t+d+N|t) \end{bmatrix} \quad \mathbf{u} = \begin{bmatrix} \Delta u(t) \\ \Delta u(t+1) \\ \vdots \\ \Delta u(t+N-1) \end{bmatrix}$$

$$\mathbf{G} = \begin{bmatrix} g_0 & 0 & \cdots & 0 \\ g_1 & g_0 & \cdots & 0 \\ \vdots & \vdots & \vdots & \vdots \\ g_{N-1} & g_{N-2} & \cdots & g_0 \end{bmatrix}$$

$$\mathbf{G}'(z^{-1}) = \begin{bmatrix} (G_{d+1}(z^{-1}) - g_0)z \\ (G_{d+2}(z^{-1}) - g_0 - g_1z^{-1})z^2 \\ \vdots \\ (G_{d+N}(z^{-1}) - g_0 - g_1z^{-1} - \cdots - g_{N-1}z^{-(N-1)})z^N \end{bmatrix}$$

$$\mathbf{F}(z^{-1}) = \begin{bmatrix} F_{d+1}(z^{-1}) \\ F_{d+2}(z^{-1}) \\ \vdots \\ F_{d+N}(z^{-1}) \end{bmatrix}. \quad (12)$$

The last two terms in (11) depend on the past and can be grouped into $\boldsymbol{f}$ leading to:

$$\mathbf{y} = \mathbf{G}\mathbf{u} + \mathbf{f}. \quad (13)$$

*3) Control Law:* The expression of the cost function to be minimized is defined as:

$$\begin{aligned} J(N, N_u) = &\sum_{j=1}^{N} \delta(j)[\hat{y}(t+j|t) - w(t+j)]^2 + \cdots \\ &+ \sum_{j+1}^{N_u} \lambda(j)[\Delta u(t+j-1)]^2, \end{aligned} \quad (14)$$

where $N$ is the prediction horizon, representing the predicted process outputs for the future $N$ time samples, $N_u$ is the control horizon, representing the future control signals for the future $N_u$ time samples, $\delta(j)$ and $\lambda(j)$ are weighting sequences, and $w(t+j)$ is the future reference trajectory. By minimizing $J$, the aim is to minimize the difference between the predicted and the reference output, and at the same time, to minimize the control effort made for error reductions.

Expression (14) can be expressed in matrix form as

$$J = (\mathbf{G}\mathbf{u} + \mathbf{f} - \mathbf{w})^T(\boldsymbol{G}\boldsymbol{u} + \mathbf{f} - \mathbf{w}) + \lambda\mathbf{u}^T\boldsymbol{u}, \quad (15)$$

where $\boldsymbol{w} = [w(t+d+1), w(t+d+2), \cdots, w(t+d+N)]^T$.

Assuming that there are no constraints on the control signals, the minimum of $J$ can be found by making the gradient of J equal to zero, which leads to:

$$\mathbf{u} = (\mathbf{G}^T\mathbf{G} + \lambda\mathbf{I})^{-1} + \mathbf{G}^T(\mathbf{w} - \mathbf{f}). \quad (16)$$

Then the first element of vector $\mathbf{u}$ is taken as the present control signal that is actually sent to the process.

*4) Parameters of the GPC Controller:* The simplified linear process model was identified around the steady-state operation of the power plant at 83% (500 MW) of its nominal load using the power plant simulator.

Having the control system for the attemperator valve operating on manual (PI controller disconnected), a step signal was applied to the process. The values resulting from the test, of the output variable (steam temperature) from the final SH were recorded.

This data was further used to identify the polynomials $A$ and $B$, which define the CARMA model. The model was discretized using a sampling time $T_s = 0.1$ s and the following expression was obtained:

$$\begin{aligned} &(1 - 0.2412z^{-1} - 0.5614z^{-2} - 0.3602z^{-3} + \\ &0.1686z^{-4})y(k) = \\ &z^{-48}(-0.0301 + 0.0073z^{-1} + 0.0169z^{-2} - 0.0516z^{-3} - \\ &0.0131z^{-4})u(k-1). \end{aligned} \quad (17)$$

From (17), we can see the result is that the model is of rank 4 and the dead time $d$ from (1) is 4.8 s.

The parameters of the GPC controller were tuned using an automatic trial-and-error procedure and the following values were found to give the best performance:

1) prediction horizon $N = 5$;
2) control horizon $N_u = 5$;
3) control weight $\lambda = 300$;
4) output weight $\delta = 1$.

## V. Simulation Tests and Anaysis

### A. PI Parameters

The parameters defining the outer loop PI controller are: $K_p = 0.5; T_i = 90$.

The parameters defining the inner loop PI controller are: $K_p = 0.012; T_i = 70$.

All parameters were tuned by experienced plant engineers, and are considered to be the best set of parameters that can be obtained.

### B. Simulation Tests

For all tests run in the simulator, the initial conditions considered were the steady-state operation of the power plant at 83% load (500 MW). During all three simulation tests, the set-point value/reference for the steam temperature was 570°C.

For the first test, the disturbance was a step load change signal from 83% (500 MW) to 100% (600 MW) nominal load. The power plant load change rate was 10 MW/min. The results of the test are shown in Fig. 7 and Fig. 8.

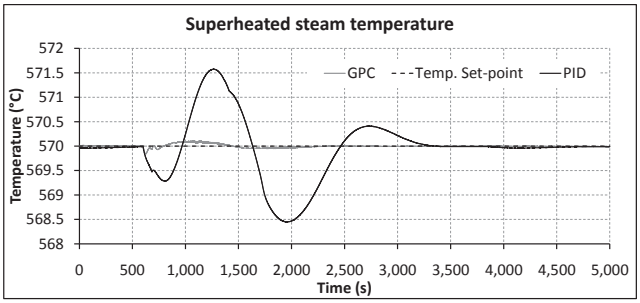


Fig. 7. Superheated steam temperature response.

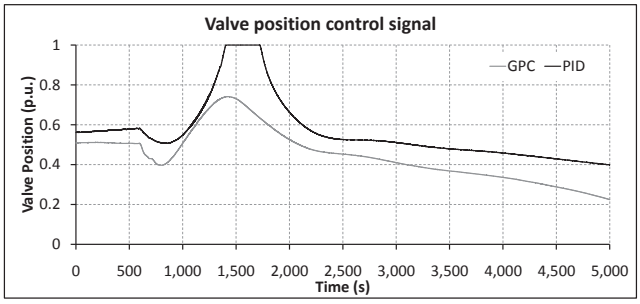


Fig. 8. Control signal variation.

The results of this test show a reduced variation range of the steam temperature for the case when the GPC controller is used. A comparative numerical analysis is given below:

PI: peak error −1.55–1.57 °C;
standard deviation 0.62 °C;
settling time 4500 s.

GPC: peak error −0.16–0.11 °C;
standard deviation 0.03 °C;
settling time 2300 s.

During the test, the average values for the valve opening area were 0.57 p.u. when the PI controller was used, and 0.45 p.u. when the GPC controller was in operation.

Based these results, it can be seen that there is a smaller over/undershoot in the temperature and the system reaches steady-state two times faster with the GPC controller in operation. A closer analysis of the control signal shows that the PI signal has significant transients, while the GPC signal is smoother.

In the second test, the load demand signal had an initial ramp up trend from 83% to 100% nominal load, with 10 MW/min load change rate; then it remained constant for 20 min and followed a ramp down trend from 100% to 83% nominal load with the same load change rate. The results obtained after this disturbance signal were then applied to the power plant and are illustrated in Fig. 9 and Fig. 10.

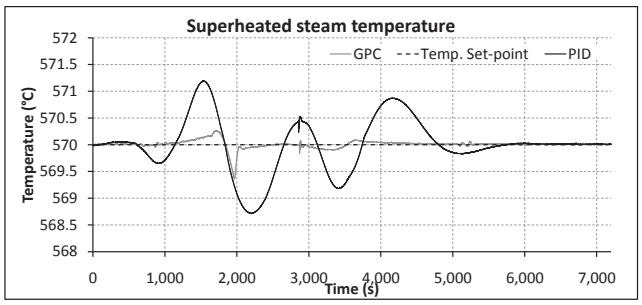


Fig. 9. Superheated steam temperature response.

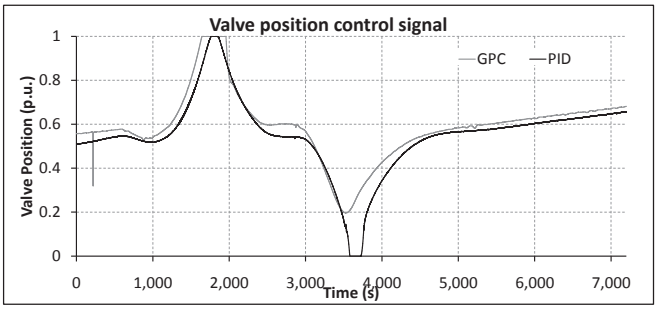


Fig. 10. Control signal variation.

The steam temperature shows again smaller variation, when the GPC controller is used. This is reflected by the numerical results given below.

PI: peak error −1.28–1.19 °C;
standard deviation 0.5 °C;
settling time 6100 s.

GPC: peak error −0.64–0.26 °C;
standard deviation 0.08 °C;
settling time 4800 s.

During the test, the average value for the valve opening area is 0.55 p.u. when the PI controller was used, compared to 0.59 p.u. when the GPC controller was in operation.

Analyzing the values for the peak error and the standard deviation, a smaller over/undershoot temperature can be seen,

along with a 21% shorter settling time for the system when the GPC controller is in operation.

Again, the control signal sent by the GPC controller is free of transients, compared to the one sent by the PI controller. The power plant modeled by the simulator is considered to have six coal mills, five in operation, and one in stand-by.

The disturbance considered for the third test was a sudden stop of one of coal mills. This affects the combustion process, which results in a variation of the flue gas temperature and this, in turn generates disturbances of the steam temperature. The results of the test are presented in Fig. 11 and Fig. 12.

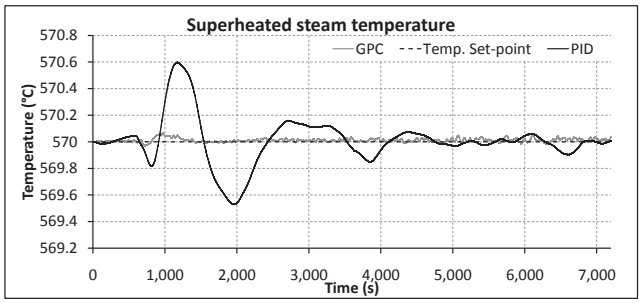


Fig. 11. Superheated steam temperature response.

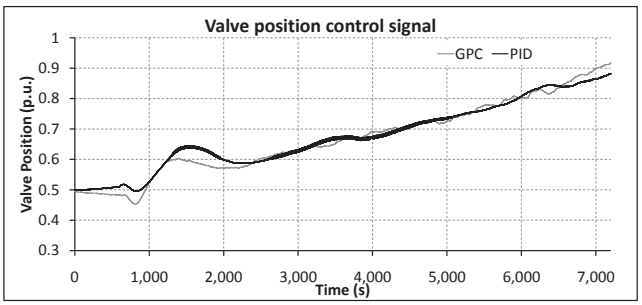


Fig. 12. Control signal variation.

Fig. 11 shows a reduced variation range of the steam temperature, when the GPC controller is tested. The graphic results are backed by the numerical data given below.

PI: peak error −0.47–0.6 °C;
standard deviation 0.18 °C;
settling time 4800 s.

GPC: peak error −0.03–0.07 °C;
standard deviation 0.01 °C;
settling time 1400 s.

During the test, the average for the valve opening area is 0.68 p.u. when the PI controller is used, compared to 0.67 p.u., with the GPC controller in operation. Regarding the water flow rate, the average is 30.94 t/h using the PI controller and 30.32 t/h with the GPC controller. The average value of the control signal is very similar, but as it can be observed from Fig. 12, the signal sent by the PI controller has considerable transients compared to the GPC one. The settling time is improved by 70% with the GPC controller in operation.

## VI. Conclusion

Judging by results obtained from simulation tests of different control strategies, the control performance of the GPC controller is seen as better than the PI controller. A numerical analysis shows that the PI performance is good, but it needs to be noted that this performance may deteriorate further due to numerous disturbances that appear in a field-operating power plant and that cannot be taken into account in a simulation environment. The GPC controller achieves a better control of the superheated steam temperature with a more stable control signal, lacking the transients that might degrade the operation of the valve actuator. The settling time is shorter as well, which means less thermal stress for the equipment, considering that the period of time when operating outside the set-point temperature is shortened.

## Appendix

TABLE AI
Boiler Specifications

| Name | Value | Unit |
|---|---|---|
| Generated power | 600 | MW |
| Superheated steam flow | 1,733 | t/h |
| Fuel flow | 276 | t/h |
| Water flow | 1,913 | t/h |
| Main steam pressure | 25.4 | MPa |
| Reheat steam pressure | 4.16 | MPa |
| Main steam temperature | 571 | °C |
| Reheat steam temperature | 569 | °C |
| Load ramping | 72 | MW/min |
| Pressure rate of change | 0.3 | MPa/min |
| Governor droop | 5 | % |

TABLE AII
Definition of the Variables Used in the Model

| Variable Name | Definition | Unit |
|---|---|---|
| $w_{\neg air}$ | Primary air flow | kg/s |
| $w_{\neg rc}$ | Raw coal flow rate | kg/s |
| $w_f$ | Pulverized coal flow rate | kg/s |
| $w_{fw}$ | Feedwater flow rate | kg/s |
| $w_1, w_2, w_3$ | Intermediate mass flow rate | kg/s |
| $w_{ms}$ | Main steam flow rate | kg/s |
| $w_{hp}$ | Steam flow rate from HP turbine to reheater | kg/s |
| $w_{rh}$ | Steam flow rate from reheater to IP turbine | kg/s |
| $Q_e, Q_{ww}, Q_{sh}, Q_{rh}$ | Heat transferred from the tube wall to the fluid | MJ/s |
| $P_{hp}$ | Mechanical power from HP turbine | MW |
| $P_{ip}$ | Mechanical power from IP turbine | MW |
| $P_{mech}$ | Mechanical power | MW |
| $f$ | Frequency | Hz |
| $P_e$ | Electrical power | MW |
| $K_e, K_{sh}, K_{ww}, K_{rh}$ | Control gains for economizer, superheater, reheater, water flow | |

## REFERENCES


[1] J. Hlava, "Model predictive control of the superheater temperature based on a piecewise affine model," in *UKACC International Conference on Control, IET*, 2010, pp. 1–10.

[2] X. Fu, D. Jiang, and Y. Zhou, "Model identification and predictive control of steam temperature in coal-fired power plant," in *International Conference on Power, Energy and Control (ICPEC)*. IEEE, 2013, pp. 509–513.

[3] C. Ziems and H. Weber, "Effects of wind turbine generated power fluctuations to thermal power generation," in *IFAC Symposium on Power Plants and Power Systems Control*, Tampere, Finland, July 2009, pp. 111–112.

[4] S. W. Sung, J. Lee, and I. B. Lee, *Process Identification and PID Control*, New York: Wiley, 2009.

[5] B. Gough, "Advanced control of steam superheat temperature on a utility boiler," Universal Dynamics Technologies Inc., Richmond, Canada, 2000.

[6] C. E. Garcia, D. M. Prett, and M. Morari, "Model predictive control: theory and practice-a survey," *Automatica*, vol. 25, no. 3, pp. 335–348, 1989.

[7] J. Richalet, A. Rault, J. Testud, and J. Papon, "Model predictive heuristic control: Applications to industrial processes," *Automatica*, vol. 14, no. 5, pp. 413–428, 1978.

[8] C. E. Garcia and A. Morshedi, "Quadratic programming solution of dynamic matrix control (QDMC)," *Chemical Engineering Communications*, vol. 46, no. 1-3, pp. 73–87, 1986.

[9] D. W. Clarke, C. Mohtadi, and P. Tuffs, "Generalized predictive control–Part I. The basic algorithm," *Automatica*, vol. 23, no. 2, pp. 137–148, 1987.

[10] P. Marquis and J. Broustail, "SMOC, a bridge between state space and model predictive controllers: application to the automation of a hydrotreating unit," in *Proceedings of the IFAC Workshop on Model Based Process Control*, 1988, pp. 37–43.

[11] W. Kim, U. C. Moon, K. Y. Lee, W. H. Jung, and S. H. Kim, "Once–through boiler steam temperature control using dynamic matrix control technique," in *Power and Energy Society General Meeting, IEEE*, 2010, pp. 1–6.

[12] A. Sanchez Lopez, G. Arroyo Figueroa, and A. Villavicencio Ramirez, "Advanced control algorithms for steam temperature regulation of thermal power plants," *International Journal of Electrical Power & Energy Systems*, vol. 26, no. 10, pp. 779–785, 2004.

[13] O. Mohamed, J. Wang, B. Al Duri, J. Lu, Q. Gao, Y. Xue, and X. Liu, "Predictive control of coal mills for improving supercritical power generation process dynamic responses," in *Proceedings of the IEEE Conference on Decision and Control*. IEEE, 2012, pp. 1709–1714.

[14] D. W. Clarke, "Application of generalized predictive control to industrial processes," *IEEE Control Systems Magazine*, vol. 8, no. 2, pp. 49–55, 1988.

[15] E. F. Camacho and C. B. Alba, *Model Predictive Control*, Berlin: Springer, 2007.

[16] T. Moelbak, "Advanced control of superheater steam temperatures–an evaluation based on practical applications," *Control Engineering Practice*, vol. 7, no. 1, pp. 1–10, 1999.

[17] J. L. Wei, J. Wang, and Q. H. Wu, "Development of a multisegment coal mill model using an evolutionary computation technique," *IEEE Transactions on Energy Conversion*, vol. 22, no. 3, pp. 718–727, 2007.

[18] O. Mohamed, J. Wang, and A. D. B, "Electrical engineering and applied computing," in *Lecture Notes in Electrical Engineering*, springer, July 2011.

[19] Y. G. Zhang, Q. H. Wu, J. Wang, G. Oluwanda, D. Matts, and Z. X. X, "Coal mill modeling by machine learning based on on-site measurement," *IEEE Transactions on Energy Conversion*, vol. 17, no. 4, pp. 549–555, 2002.

[20] Y. N. Yu, *Electric Power System Dynamics*, Academic Press, 1983.

[21] E. B. Woodruff, H. B. Lammers, and T. F. Lammers, *Steam Plant Operation*, McGraw-Hill, 2004.

[22] S. W. Sung, J. Lee, and I. B. Lee, *Process Identification and PID Control*, New York: Wiley, 2009.

[23] K. M. Yu and J. A. Kim, "Model reference PID control and tuning for steam temperature in thermal power plant," in *11th International Conference on Control, Automation and Systems (ICCAS)*. IEEE, 2011, pp. 415–419.

[24] D. CLARKE, C. MOHTADI, and P. Tuffs, "Generalized predictive control Part II. Extensions and interpretations," *Automatica*, vol. 23, no. 2, pp. 149–160, 1987.


**Mihai Draganescu** received his B.Eng. in power systems engineering and M.Sc. in electromagnetic compatibility and power quality from Faculty of Power Engineering, University Politehnica of Bucharest, Bucharest, Romania in 2005 and 2007, respectively. He is a Ph.D. degree candidate at the University of Warwick. His current research interests are power plant control system, model predictive control algorithms, nonlinear programming and intelligent control.

**Shen Guo** received the B.Eng. degree in electrical engineering from Wuhan University, China, in 2006. He received the M.Sc. degree in system monitoring from the University of Birmingham in 2009. He is currently a Ph.D. student in the School of Engineering, University of Warwick. His research interest include coal mill modeling, power plant modeling and control, post-combustion carbon capture technologies and applications of evolutionary computation algorithms.

**Jacek D Wojcik** received his M.Sc. and Ph.D. degrees in electrical engineering from the Wroclaw University of Technology, Poland, in 2002 and 2007, respectively. Currently, he is a Research Fellow in the School of Engineering at the University of Warwick, U.K. His research interest covers thermal power plants: modeling, simulations and control, power system analysis, and renewable energy sources integration with the grid.

**Jihong Wang** received the B.Eng. degree from Wuhan University of Technology, China, in 1982, the M.Sc. degree from Shandong University of Science and Technology, Jinan, China, in 1985, and the Ph.D. degree from Coventry University, Coventry, U.K., in 1995. She is currently a professor with the School of Engineering, University of Warwick. Her research interests include nonlinear system control, system modeling and identification, power systems, energy efficient systems, and applications of intelligent algorithms.

**Xiangjie Liu** received his Ph.D. degree in electrical and electronic engineering from Northeastern University, China, in 1997. He subsequently held a postdoctoral position with the China Electric Power Research Institute, Beijing, China, until 1999, after which he has been a associate professor since 1999. After he worked as a research associate with the University of Hong Kong, he became a professor at the National University of Mexico in 2001. He is now a professor with the Department of Automation, North China Electric Power University, China. His current research areas include fuzzy control, neural networks, adaptive and predictive control, intelligent control theory, and application in industrial process.

**Guolian Hou** received the bachelor's, master's and Ph.D. degrees, all from North China Electric Power University in 1988, 1990, and 1997 respectively. She is a professor in the Department of Automation at North China Electric Power University, Beijing, China. She was with the Department of Electrical Engineering and Electronics, at Liverpool University, U.K. as a visiting scholar from May 2005 to Nov 2006. Her research interests include fuzzy control, power system, and multi-agent.

**Yali Xue** received her Ph.D. in control engineering from Tsinghua University, Beijing, China. She currently holds a researcher position at the Department of Thermal Engineering, Tsinghua University, Beijing, China. Her research areas are control, operation and modeling of fossil power plant.

**Qirui Gao** received his Ph.D. in thermal engineering from Tsinghua University, Beijing, China. He is now a vice professor at the Institute of Thermal Dynamic Simulation & Control, Department of Thermal Engineering, Tsinghua University, Beijing, China. His research interests are thermal dynamic simulations and process modeling.